Subtopic: Laminar Flames ID: 128LF-0138

12th U.S. National Combustion Meeting May 24-26, 2021, College Station, Texas

Two-dimensional simulation of cool and double flame formation induced by the laser ignition under shock-tube conditions

Tianhan Zhang^{1*}, Adam J. Susa², Ronald K. Hanson², Yiguang Ju¹

¹Department of Mechanical and Aerospace Engineering, Princeton University, NJ

² Department of Mechanical Engineering, Stanford University, CA

*Corresponding Author Email: tianhanz@princeton.edu

The laser ignition-induced spherical double flame's initiation, propagation, and transition are studied using n-heptane/O₂/Ar/He mixture by two-dimensional simulation with the detailed mechanism. The current study's primary goal is to reveal how the turbulent flow field after the laser ignition leads to the double flame formation and further affects the flame propagation. The results show that a pure cool flame or a double flame can be formed at shock-tube conditions depending on the laser pulse energy. The over-driven shock wave after the laser spark significantly distorts the temperature field and the radical spatial distribution. For the laser energy large enough, a torus-like shape hot flame is ignited at the ignition kernel center. Shortly after, a cool flame is formed at the outer surface of the hot flame. Therefore, a two-dimensional, transient premixed double flame structure is observed. The outer cool flame can coexist with the hot flame for a long time, dramatically accelerating the hot flame propagation and fundamentally impacting the flame speed interpolation. To further investigate the double flame formation, effects of ignition energy, laser spark shape, initial temperature, low-temperature chemistry, and the ignition Damkohler number are studied. The present study provides essential physical insight and guidance for the flame speed measurement using laser ignition at engine-relevant conditions.

Keyword: laminar flame, cool flame, double flame, laser ignition

1. Introduction

Due to growing concerns over worldwide air pollution and energy sustainability, there is an increasing interest to develop advanced compression-ignition engines, such as homogeneous charge compression-ignition (HCCI) engines[1], reactivity-controlled compression ignition engines (RCCI)[2], and spark assisted HCCI engines[3]. The advanced engines adopt higher temperature and pressure to increase the compression ratio, thus boosting combustion efficiency. At such conditions, characteristic timescales of low- and high-temperature autoignition are significantly reduced. As a result, autoignition, cool flame, and hot flame are inherently coupled and become critical for understanding the flame dynamics under the engine conditions fully.

Cool flames have been studied experimentally using many different burners, including heated burners[4], stirred reactors[5], counterflow burners[6], and rapid compression machines[8]. Besides, planar propagating cool flames[9], and spherically propagating cool flames[10] are studied numerically. A recent review of the cool flame dynamics provides a comprehensive summary of the cool flame field's accumulated progress [11]. The studies showed several flame regimes, including cool flame, warm flame, hot flames. Besides, cool and hot flames can coexist under certain conditions and form the so-called double flame structure. Unfortunately, most of

these studies focused on the low initial temperature and one-dimensional geometry. Very few studies investigate the cool and double flame dynamics at high temperature, engine-related conditions, especially coupling between flames and the flow field. Susa et al. measured the flame speed over a wide range of temperature using shock-tube experiments[12]. The results showed the non-monotonic dependence of the flame speed on temperature in the negative temperature-coefficient (NTC) region. The results suggested that cool flames and low-temperature chemistry play an essential role to flame propagation under engine-related conditions.

There are extensive efforts on cool and double flame modeling. Ju et al. were the first to identify the cool and hot flame coexistence in high-pressure spark-assisted HCCI engine conditions[13]. Ju et al.[14] further investigated the effects of pressure, heat loss, and equivalence ratio. Zhao studied the initiation and propagation of the premixed cool flames using DME/O2/N2 mixtures[15]. Pan et al. studied the flame propagation speed affected by the low-temperature ignition near the negative temperature coefficient region[16]. Zhang et al. modeled the transient planar premixed cool and double flames[17]. Zhang and Ju systematically studied the structures, and the flame speed of the autoignition assisted cool and warm flames under a wide range of temperature, pressure, and equivalence ratio[18]. Based on Susa et al. shock-tube experiments, Zhang et al. modeled the autoignition-assisted spherical cool and double flames formation and propagation[10]. It pointed out that depending on the low-temperature ignition Damkohler number, the cool flame can merge into or split from the hot flame. The single flame to double flame transitions lead to new regimes for the spherical flame propagation and explains the nonmonotonic flame speed trend. Unfortunately, the previous studies modeled the cool and double flame using one-dimensional spherical coordinate, which is not able to model the couplings between the cool, hot, and double flame formation and transition with the high dimensional flow fields. In particular, the laser ignition leads to turbulent flow motions and results in lobe-shaped flame kernels. The transient evolvement of the flame kernel and the impact on the flame propagation were largely ignored by the previous studies.

The current study's primary goal is to investigate the effects of the laser ignition and the consequent plasma and flow fields on the cool and double flame structure, propagation, and chemical kinetics using different laser energies at different initial temperatures. To highlight the effects of the laser-induced plasma and flow fields on the cool flame formation and propagation, a pure cool flame case is first demonstrated. Then, the second case shows the unsteady double flame formation. Furthermore, to illustrate the importance of the low-temperature chemistry, another simulation case with the initial temperature higher than the negative temperature region is performed and compared with the previous cases. Finally, conclusions are drawn.

2. Numerical method

In the present study, n-heptane/O₂/Ar/He is chosen as the mixture due to its low-temperature chemistry and being the major component of the Primary Reference Fuel (PRF). In addition, a nominal oxidizer composition of 0.18 O₂, 0.41 Ar, 0.41 He is used in this work to remain the same mixture conditions with the shock-tube experiments. A reduced n-heptane/O₂/Ar/He mechanism with 70 species is generated by the Path Flux Analysis (PFA)[19] from a detailed mechanism[20]. To provide the chemiluminescence information, an additional OH* mechanism is added in the mechanism[21]. The two-stage autoignition delay times for n-heptane/O₂/Ar/He at P = 1 atm, ϕ = 0.9 are calculated using the reduced mechanism. Since the laser ignition can induce initial plasmas, the ignition might be significantly accelerated. For reference, at T = 700 K, the low-temperature and high-temperature ignition delay times are 6.08 ms and 0.42 s,

respectively. With 1E-7 and 1E-5 mole fraction OH radical addition, the low-temperature ignition delay times are accelerated to 2.88 ms and 1.45 ms.

The in-house code Multiscale Adaptive Reduced Chemistry Solver (MARCS) is used for the high-dimensional transient flame simulations. The solver uses the 4th order Runge-Kutta scheme in time and the 3rd order AUSMPW+ scheme in space. To improve computation efficiency, the hybrid multi-timescale (HMTS) method is adopted[22]. Besides, the solver also implements the adaptive mesh refinement (AMR) algorithm[23]. The refinement criterion is based on the temperature, pressure, and density gradient. The base cell size is 0.5 mm, and the minimum cell size is eight µm. The grid convergence is performed to guarantee accuracy.

The shock tube and the Nd: YAG laser apparatuses are illustrated in Figure 1b. Laser ignition is usually composed of five stages: electrical breakdown, shock-wave formation, lobe formation, ignition, and flame propagation. The current work mainly focuses on the hydrodynamic effects induced by the laser spark. As a result, the laser energy absorbed by the mixture is modeled, focusing on the spatial temperature distribution, especially asymmetric absorption in the laser-beam direction. The energy distribution is fitted to the axisymmetric Gaussian distribution in the direction normal to a laser beam and can be expressed as[24]:

$$I(r,z,t) = \frac{A}{\pi r_0^2 [1 + C(z+z')^2]} \exp \left[-\frac{\left(\frac{r}{r_0}\right)^2}{1 + C(z+z')^2} \right] \exp \left[-\frac{\left(t - \frac{\tau_s}{2}\right)^2}{\tau_0^2} \right]$$

Where A and C are constants based on the previous experimental data.

Since the laser energy distribution only depends on r and z, independent of azimuthal angle, the simulation can be considered a rotation-symmetrical problem. To improve the computation efficiency, a two-dimensional cross-section is chosen as the simulation domain. The bottom boundary uses the symmetry boundary condition, and the other three boundaries use the outlet boundary condition. The domain size is from 8 mm * 16 mm to 20 mm * 40 mm. The initial temperature is chosen as 700 K and 900 K, and the laser pulse energy varies from 1 mJ to 10 mJ approximately.

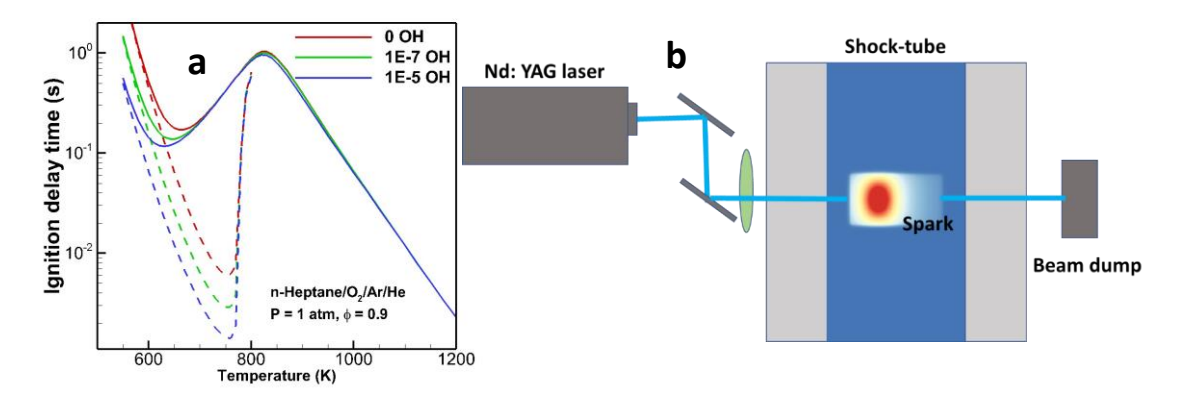


Figure 1 a). Ignition delay time for n-heptane/ O_2 /Ar/He mixture at P = 1 atm, T = 550-1200 K, ϕ = 0.9 with and without OH additions. b). Experimental apparatus for the shock tube and laser ignition. Illustration for the simulation domain.

3. Results and discussion

3.1. Small laser ignition energy: cool flame only

Figure 2 shows the early stages of a laser ignition process. In Figure 2a, at $t=0.5~\mu s$, an extremely high temperature and pressure region are generated by a laser spark. The temperature is above 7500 K, and the pressure is above 10 atm. Shortly after, a strong, over-driven shock wave is formed at $t=1~\mu s$, as shown in Figure 2b. Then, the shock wave perturbation and the asymmetrical laser energy absorption led to a highly turbulent flow field near the laser spark center. Afterward, a distorted flame kernel is formed and starts to propagate. Figure 2d shows the kinetic energy distribution and the velocity vector near the flame kernel at $t=2~\mu s$. There are two large clockwise vortices. The initial flow velocity is around $1{\sim}10~m/s$, larger than the flame propagation speed. As a result, the initial flame kernel evolvement is mainly affected by the turbulent flow motion.

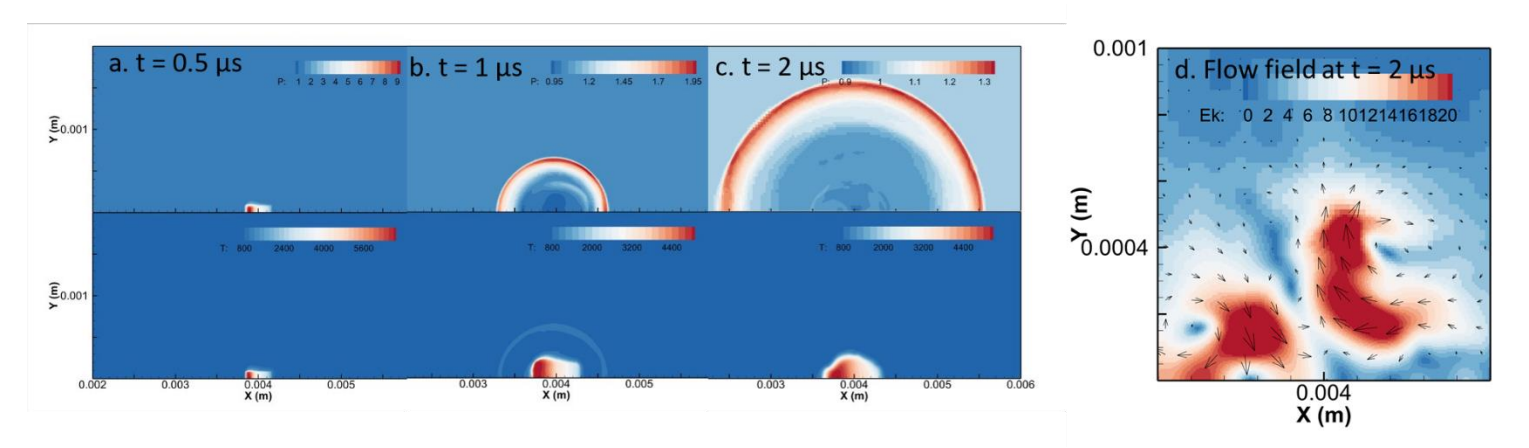


Figure 2. a-c: pressure and temperature contours for the laser induced shock wave and flame kernel at time = 0.5, 1, 2 μ s, respectively for n-heptane/ O_2 /Ar/He mixture at P = 1 atm, T = 700 K, ϕ = 0.9. d: corresponding kinetic energy distribution and velocity field near the flame kernel at 2 μ s.

Figure 3 shows flame propagation process using a small laser energy pulse at T=700~K, P=1~atm, $\phi=0.9$. Since the laser energy is so small that it is below the hot flame's minimum ignition energy, only a small region of the premixed mixture is ignited at $t=60~\mu s$. The hot flame keeps losing heat and radicals until it extinguishes at around $t=600~\mu s$. Figure 3e shows the flow motion at the same time. It is interesting to note that even though the hot flame is extinguishing, the remaining radicals are transported by the vortices and moves to the neighboring low-temperature domain. At around $t=2000~\mu s$, a cool flame is formed away from the previous hot flame locations. The cool flame formation is three times quicker than the low-temperature ignition delay time. The main reason is the cool flame takes advantage of the radicals generated near the laser spark and the hot flame front. For example, the transported OH radical mole fraction is around 1E-6 to 1E-7. The cool flame formation time is comparable to the autoignition delay time with a similar level of OH additions. At $t=3300~\mu s$, a C-shape cool flame is formed. The cool flame is C-shape instead of spherical because it prefers the zones with higher radical

concentrations. Consequently, it propagates along the outer surface of the previous hot flame kernel to absorb more radicals.

Figure 4 shows the temperature, heat release rate, and radical mass fractions on the centerline X = 4 mm. The flame front temperature, peak heat release rate, the CH₂O production confirm that it is a self-sustaining cool flame.

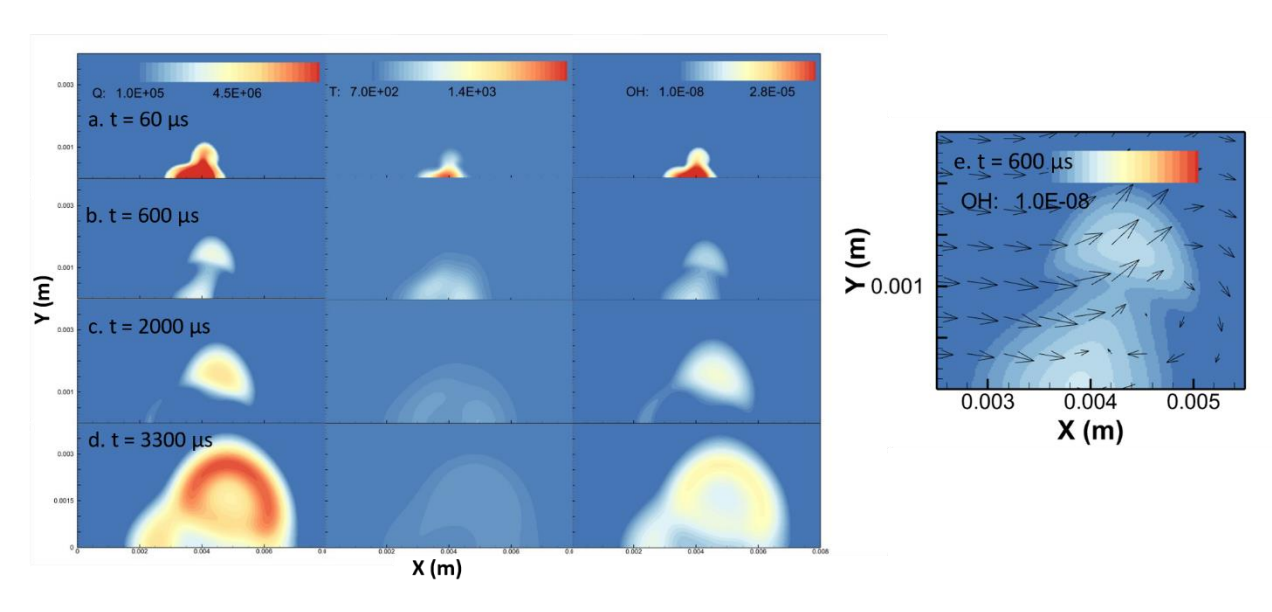


Figure 3. a-d: heat release rate, temperature, and OH concentration contours for the flame kernel at P=1 atm, T=750 K, $\phi=0.9$, laser spark energy~1 mJ,; e: velocity field at t=600 μ s.

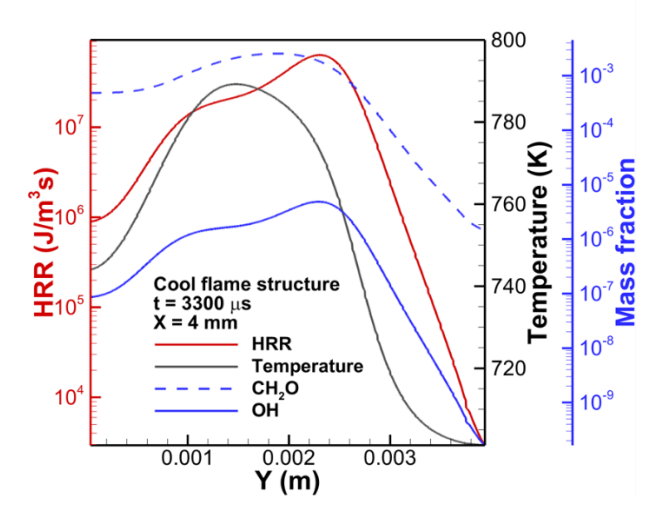


Figure 4. Cool flame structure (temperature, heat releaser rate, OH, CH2O distribution) extracted from the 2D simulation case (Figure 3) P = 1 atm, T = 750 K, $\phi = 0.9$, X = 4 mm.

The cool flame formation and propagation have several important implications. First, it demonstrates the importance of cool flame dynamics. Cool flame has a much lower requirement for ignition energy compared with a hot flame. In addition, the cool flame is more sensitive to plasma assistance. A small number of radicals can significantly accelerate cool flame formation. For the experiment design, the results provide a possible way to capture cool flame in the enginerelevant conditions using a low-energy laser pulse. Moreover, previous studies used low temperature ignition delay time as the deadline to perform a measurement to exclude the effects of the low-temperature chemistry and the cool flame. This criterion might not be accurate and needs further considerations.

3.2. Large laser ignition energy: double flame

Figure 5 shows transient flame propagation at T=700~K, P=1~atm, $\phi=0.9$ using a large laser energy pulse (around 10 mJ). Figure 5a shows that at early-stage $t=20~\mu s$, a thickened preheat zone (in white color) starts to appear in front of the hot flame front due to a pool of radicals near the laser spark. As shown in Figure 5b the preheat zone encompasses the hot flame surface. Figure 5c shows such structure can remain for several hundreds of micro-seconds. Figure 6 shows the temperature, heat release rate, and radical mass fraction distributions on the central line X=4~mm. From the heat release distribution, it is clear that there are two stages of reaction. The first one appears at $T\sim750K$. The heat release rate is $1E7~J/m^3 s$, which is a typical cool flame pattern. The second front is a hot flame front with $T\sim1600~K$, $Q\sim1E9~J/m^3 s$. As shown in Figure 5, the double flame formation is mainly attributed to the laser-induced radicals and temperature field. After the shock wave, the turbulent flow motion transports the laser-induced radicals and the heat to the adjacent domain. This process dramatically accelerates the leading cool flame formation.

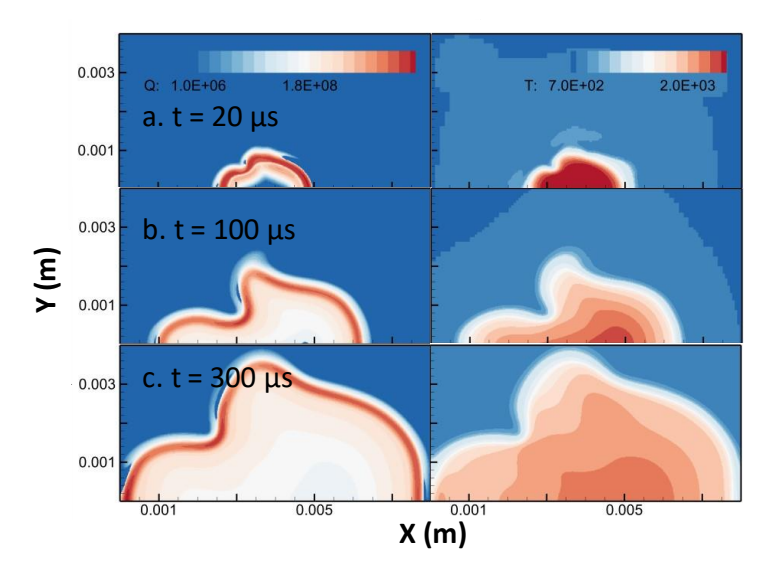


Figure 5. Heat release rate and temperature contours for the double flame at P = 1 atm, T = 750 K, $\phi = 0.9$

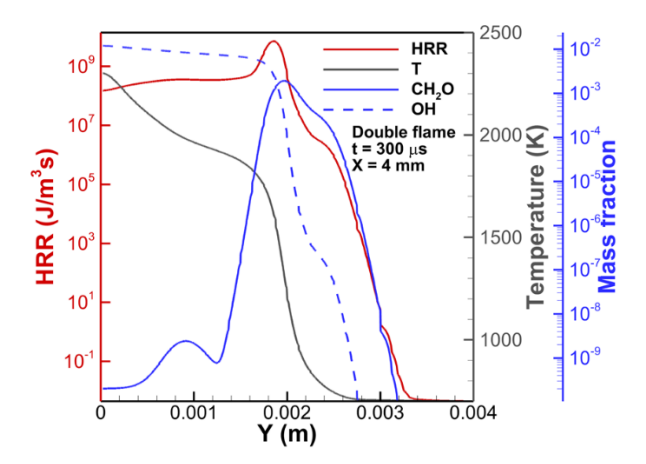


Figure 6 Double flame structure (temperature, heat releaser rate, OH, CH2O distribution) extracted from the 2D simulation case (Figure 5) P = 1 atm, T = 750 K, $\phi = 0.9$, laser spark energy~10 mJ, X = 4 mm.

4. Conclusions

The current work investigates the cool, hot, and double flame formation and propagation under the shock-tube condition with laser ignitions using two-dimensional numerical simulations. A detailed chemistry mechanism for n-heptane/ O_2 /Ar/He with OH* chemiluminescence is adopted. The effects of the over-driven shock wave, initial turbulent flow motions, laser spark energy, initial temperature, and chemical kinetics are studied. The results show that a cool flame requires much lower ignition energy than a hot flame. In a laser-ignition combustion system, the cool flame formation and low-temperature ignition can be significantly accelerated due to the laser-induced radicals and the initial turbulent flow field. The autoignition delay time needs further consideration to be used as the reference value in experimental measurement. The results also reveal the transient double flame formation process. The double flame formation is primarily affected by the laser-induced radicals. The distance between the leading cool flame and the trailing hot flame is close, while the structure can remain for a long time due to the thermal expansion and the flow convection. The current work provides essential insights to understand cool flame dynamics under engine-relevant conditions with laser ignition.

References

- [1] R.H. Thring, Homogeneous-Charge Compression-Ignition (HCCI) Engines, in: SAE Tech. Pap., SAE International, 1989.
- [2] S.L. Kokjohn, R.M. Hanson, D. a. Splitter, R.D. Reitz, Fuel reactivity controlled compression ignition (RCCI): a pathway to controlled high-efficiency clean combustion, Int. J. Engine Res. 12 (2011) 209–226.
- [3] J. Hyvönen, G. Haraldsson, B. Johansson, Operating Conditions Using Spark Assisted HCCI Combustion During Combustion Mode Transfer to SI in a Multi-Cylinder VCR-HCCI Engine, in: 2005.
- [4] H.J. Emeléus, CCCXCIV.—The spectra of the phosphorescent flames of carbon disulphide and ether, J. Chem. Soc. 129 (1926) 2948–2951.
- [5] J.F. Griffiths, T. Inomata, Oscillatory cool flames in the combustion of diethyl ether, J. Chem. Soc. Faraday Trans. 88 (1992) 3153.
- [6] C.B. Reuter, S.H. Won, Y. Ju, Experimental study of the dynamics and structure of self-sustaining premixed

- cool flames using a counterflow burner, Combust. Flame. 166 (2016) 125-132.
- [7] V. Nayagam, D.L. Dietrich, P. V. Ferkul, M.C. Hicks, F.A. Williams, Can cool flames support quasi-steady alkane droplet burning?, Combust. Flame. 159 (2012) 3583–3588.
- [8] W.S. Affleck, A. Fish, Knock: Flame acceleration or spontaneous ignition?, Combust. Flame. 12 (1968) 243–252.
- [9] Y. Ju, C.B. Reuter, S.H. Won, Numerical simulations of premixed cool flames of dimethyl ether/oxygen mixtures, Combust. Flame. 162 (2015) 3580–3588.
- [10] T. Zhang, A.J. Susa, R.K. Hanson, Y. Ju, Studies of the dynamics of autoignition assisted outwardly propagating spherical cool and double flames under shock-tube conditions, Proc. Combust. Inst. 000 (2020) 1–9.
- [11] Y. Ju, C.B. Reuter, O.R. Yehia, T.I. Farouk, S.H. Won, Dynamics of cool flames, Prog. Energy Combust. Sci. 75 (2019) 100787.
- [12] A.J. Susa, A.M. Ferris, D.F. Davidson, R.K. Hanson, Experimental Observation of Negative Temperature Dependence in iso -Octane Burning Velocities, AIAA J. 57 (2019) 4476–4481.
- [13] Y. Ju, W. Sun, M.P. Burke, X. Gou, Z. Chen, Multi-timescale modeling of ignition and flame regimes of nheptane-air mixtures near spark assisted homogeneous charge compression ignition conditions, Proc. Combust. Inst. 33 (2011) 1245–1251.
- [14] Y. Ju, On the propagation limits and speeds of premixed cool flames at elevated pressures, Combust. Flame. 178 (2017) 61–69.
- [15] P. Zhao, W. Liang, S. Deng, C.. K. Law, Initiation and propagation of laminar premixed cool flames, Fuel. 166 (2016) 477–487.
- [16] J. Pan, H. Wei, G. Shu, Z. Chen, P. Zhao, The role of low temperature chemistry in combustion mode development under elevated pressures, Combust. Flame. 174 (2016) 179–193.
- [17] W. Zhang, M. Faqih, X. Gou, Z. Chen, Numerical study on the transient evolution of a premixed cool flame, Combust. Flame. 187 (2018) 129–136.
- [18] T. Zhang, Y. Ju, Structures and propagation speeds of autoignition-assisted premixed n-heptane/air cool and warm flames at elevated temperatures and pressures, Combust. Flame. 211 (2020) 8–17.
- [19] W. Sun, Z. Chen, X. Gou, Y. Ju, A path flux analysis method for the reduction of detailed chemical kinetic mechanisms, Combust. Flame. 157 (2010) 1298–1307.
- [20] S. Dooley, F. Dryer, S.H. Won, T. Farouk, Reduced Kinetic Models for the Combustion of Jet Propulsion Fuels, in: 51st AIAA Aerosp. Sci. Meet. Incl. New Horizons Forum Aerosp. Expo., American Institute of Aeronautics and Astronautics, Reston, Virigina, 2013.
- [21] J.M. Hall, E.L. Petersen, An optimized kinetics model for OH chemiluminescence at high temperatures and atmospheric pressures, Int. J. Chem. Kinet. 38 (2006) 714–724.
- [22] X. Gou, W. Sun, Z. Chen, Y. Ju, A dynamic multi-timescale method for combustion modeling with detailed and reduced chemical kinetic mechanisms, Combust. Flame. 157 (2010) 1111–1121.
- [23] P. Macneice, K.M. Olson, C. Mobarry, R. De Fainchtein, C. Packer, PARAMESH: A parallel adaptive mesh refinement community toolkit, Comput. Phys. Commun. 126 (2000) 330–354.
- [24] M.H. Morsy, S.H. Chung, Numerical simulation of front lobe formation in laser-induced spark ignition of CH4/air mixtures, Proc. Combust. Inst. 29 (2002) 1613–1619.